# High-resolution line broadening and collisional studies in $CO_2$ using nonlinear spectroscopic techniques*

Thomas W. Meyer†‡ and Charles K. Rhodes§
*Lawrence Livermore Laboratory, University of California, Livermore, California 94550*

Hermann A. Haus
*Massachusetts Institute of Technology, Research Laboratory of Electronics and Department of Electrical Engineering, Cambridge, Massachusetts 02139*

(Received 29 October 1974; revised manuscript received 31 March 1975)

High-resolution line-broadening studies have been made of $CO_2$ in collision with a wide variety of foreign gas perturbers. These measurements have been made by observation of the narrow saturated resonance in the 4.3-$\mu$m fluorescence emitted from a low-pressure $CO_2$ gas which is subjected to a saturating standing-wave electric field from a $CO_2$ oscillator operating on a 9.6- or 10.6-$\mu$m transition. The collision partners which have been investigated are $CO_2$, $N_2O$, $N_2$, NO, CO, $O_2$, $H_2$, $D_2$, $^3He$, $^4He$, Ne, Ar, Kr, Xe, $NH_3$, and $CH_4$. A semiclassical theory of the 4.3-$\mu$m saturated resonance is developed which accounts for the effects of phase-interrupting collisions, beam transit time, and optical intensity. The observation of a previously unobserved downward curvature of the $CO_2$ linewidth data at low pressure is attributed to the influence of the transit-time effect. The experimentally determined pressure-broadening coefficients include the important correction for the contribution of power broadening. These power-corrected results for $CO_2$, $N_2$, and $^4He$ have been used to predict successfully the observed gain characteristics of high-pressure ($>1$ atm) $CO_2$ amplifiers, as observed in other studies. We have also appraised our observed broadening coefficients in the context of the pressure-broadening theory developed by Murphy and Boggs in order to characterize quantitatively the intermolecular interactions. The comparison of theroy and experiment indicates the need for an explicit incorporation of vibration perturbations in the theoretical analysis, particularly when vibrational resonance is present.

## I. INTRODUCTION

In this paper we present the results of high-resolution line-broadening studies of the linear $CO_2$ molecule in collision with a substantial variety of foreign gas perturbers. Nonlinear saturation spectroscopic methods were used to directly observe the homogeneous line shape on line center of a low-pressure $CO_2$ gas which is subjected to a saturating standing-wave electric field from a $CO_2$ oscillator. The purpose of these measurements is threefold: (i) By investigating the pressure dependence of the frequency full width at half maximum (FWHM) of the line shape, the pressure-broadening coefficient for the various collision partners may be obtained; (ii) by determining the intensity dependence of the line shape, the important contribution arising from power broadening is directly established; and (iii) through the use of an appropriate pressure-broadening theory we can investigate the detailed nature of the processes involved in intermolecular collisions by correlating the results of calculations obtained from this theory with the data of (i) above.

We proceed in the following manner: Section II describes the experimental method, while Sec. III presents details of the experimental results. A theory which describes the interaction of the laser electric field with the absorbing $CO_2$ medium is presented in Sec. IV. The results of this theory are compared with the data in Sec. V, and it is shown that the data of Sec. III must be substantially corrected for the influence of power broadening. This correction is implemented in Sec. VI, and the results are compared with the investigations of other authors. In Sec. VII we attempt to calculate our pressure-broadening results using the theoretical formulation of Murphy and Boggs. Finally, our conclusions are stated in Sec. VIII.

## II. EXPERIMENTAL METHOD

The technique applied in these studies utilizes the nonlinear method of measurement of the $CO_2$ homogeneous line shape, originated by Freed and Javan,[1] in which the 4.3-$\mu$m fluorescence arising from the $CO_2$ ($00^01-00^00$) transition is monitored from a low-pressure $CO_2$ gas which is subjected to a saturating standing-wave 9.6- or 10.6-$\mu$m $CO_2$ optical field. As the saturating laser is frequency tuned through the $CO_2$ line center, a narrow saturated resonance dip appears in 4.3-$\mu$m fluorescence. The major contributions to the FWHM of the dip include pressure-broadening, power-broadening, and transit-time effects.[2] As we have already mentioned, an investigation of the functional dependence on pressure and intensity of the FWHM of the $CO_2$ 4.3-$\mu$m saturated resonance line shape

can provide information on both the pressure-broadening coefficient of the relevant gas mixture and on the detailed nature of the nonlinear interaction with the optical field.

The experimental arrangement used to observe the line-shape measurements is illustrated in Fig. 1. Two stable, single-line $TEM_{00}$ mode $CO_2$ oscillators[3] allow individual selection of any of the $CO_2$ 9.6- or 10.6-$\mu$m rotational-vibrational transitions. A piezoelectric translator (PZT) may be used to scan each transition across its gainwidth. Both oscillators are equipped with intracavity, Brewster-window, absorption cells. The 4.3-$\mu$m fluorescence emanating from a gaseous mixture of $CO_2$ and some perturber ($M$) contained in the absorption cell is collected by a large Au mirror in the bottom of the cell and focused through a sapphire window in the top of the cell into a nitrogen-cooled In:Sb detector. The derivative of the fluorescence is detected synchronously with a lock-in amplifier by applying a sinusoidal ac modulation of frequency $\omega$ ($\omega \approx 1$ kHz) to the PZT on which the output mirror is mounted.

One oscillator (2) is formed into a local oscillator by locking it to the line center of a low-pressure (30 mTorr) $CO_2$ gas with a stability of 3 parts in $10^{10}$. Both oscillators (1, 2) have linewidths of ~20 kHz. Oscillator (1) is used to probe the gas ($CO_2 + M$) of interest and its output is heterodyned with that of the local oscillator (2) in a helium-cooled Cu:Ge detector. The output of this detector leads to a counter wherein the frequency measurement $|(\omega_1 - \omega_2)|$ is established. The 4.3-$\mu$m fluorescence data from the probe oscillator (1) is recorded on magnetic tape simultaneously with the heterodyne signal between the probe and reference oscillators as the former is swept in frequency from −10 to +10 MHz by applying a dc ramp voltage to its PZT.

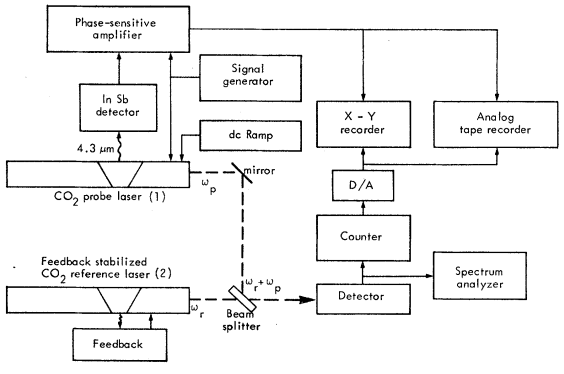


FIG. 1. Experimental arrangement used to make $CO_2$ line-shape measurements. 4.3-$\mu$m fluorescence signal originates from the intracavity absorption cell of the probe laser (1).

## III. EXPERIMENTAL RESULTS

After the fluorescence data are recorded on magnetic tape they are computationally processed by first integrating them and then numerically least-squares fitting the resulting fluorescence intensity. The fitting curve consists of a Lorentzian to match the saturated line shape and a second-order curve to fit the background, which is comprised of the Doppler absorption profile of the gas convolved with the broad power variation of the probe laser. Typical results using this method appear in Fig. 2 for 75-mTorr pure $CO_2$. The experimental data are given by the solid line, and the dotted line is the numerical fit to the data. The dashed curve in Fig. 2 is the computer generated background signal accounting for the absorption which does not participate in the interference phenomenon causing the Lamp dip. If the background is subtracted from the data, the homogeneous line shape is obtained as shown by the solid curve in Fig. 3. The dotted curve is the Lorentzian fit to the line shape, and it is evident from Fig. 3 that this is an excellent description of the data. Results of this nature are typical and are found over the full range of pressures and collision partners examined in these experiments.

A plot of the frequency (FWHM) of the line shape as a function of pressure for $CO_2$ in collision with the perturbers $CO_2$, $N_2$, $H_2$, $D_2$, $^4He$, and Xe is

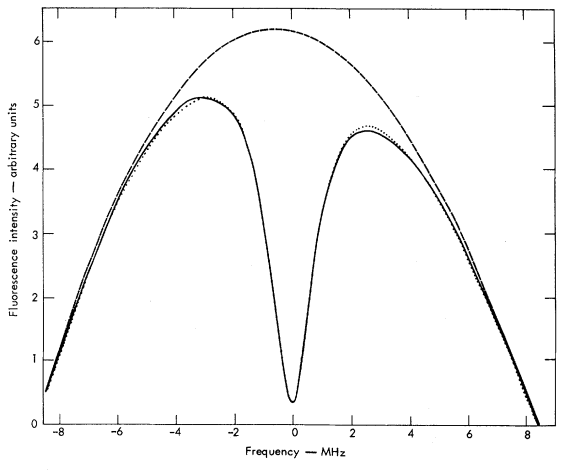


FIG. 2. Integrated 4.3-$\mu$m $CO_2$ fluorescent intensity depicting the saturated resonance feature (lower solid curve). Dotted curve is a computer fit to the data, and the upper dashed curve is a computer generated background. $CO_2$ pressure is 75 mTorr.

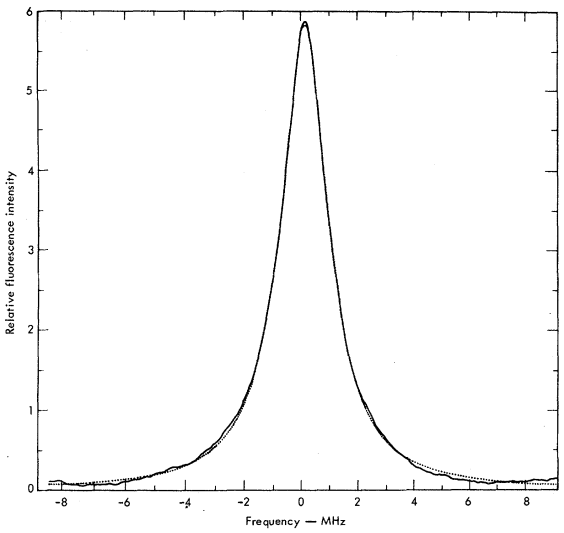


FIG. 3. Saturated resonance line shape (solid wavy curve) obtained from Fig. 2 by subtracting the background from the data. Smooth dotted curve is a Lorentzian, which has the same FWHM as the data.

given in Fig. 4 for the 10.6-$\mu$m $P(20)$ transition. A similar representation of the 9.6-$\mu$m $P(20)$ data appears in Fig. 5. Each FWHM point is the average of four sets of data at that pressure. The partial pressure of $CO_2$ in all cases is 30 mTorr, and the gas pressures were accurately measured with a Barocell capacitive manometer. As an added precaution, gas mixtures were sampled at various pressures and then analyzed with a mass spectrometer. In every sample the mass-spectrometer results agreed to within < 1% of the partial pressures obtained with the manometer. Only research-grade gases were used in the experiment.

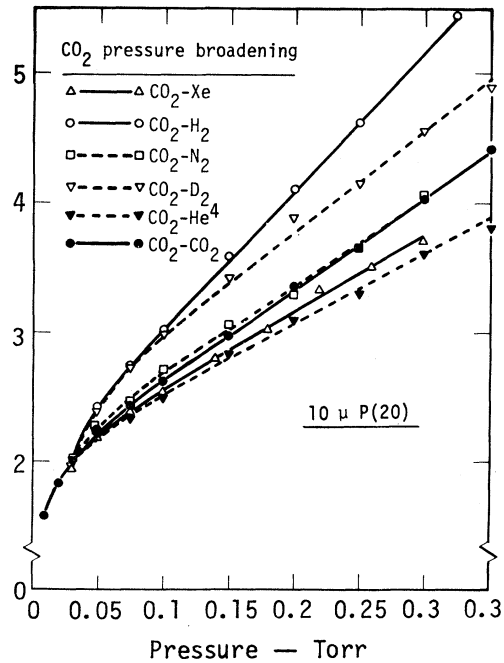


FIG. 4. $CO_2$ pressure-broadening data on the 10.6-$\mu$m $P(20)$ transition for the collision partners $H_2$, $D_2$, $CO_2$, $N_2$, Xe, and $He^4$.

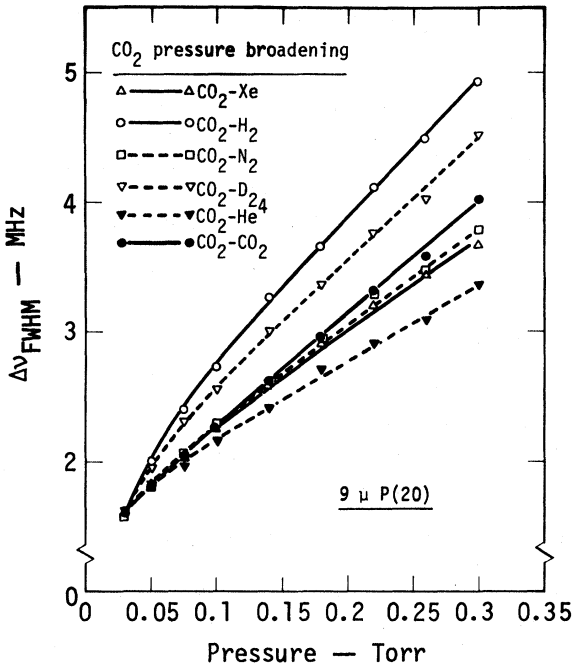


FIG. 5. $CO_2$ pressure-broadening data on the 9.6-$\mu$m $P(20)$ transition for the collision partners $H_2$, $D_2$, $CO_2$, $N_2$, Xe, and $He^4$.

Note that each of the curves of Figs. 4 and 5 exhibit two distinctive features. First, there is a linear portion extending from around 100 mTorr to the highest pressure measured (300–350 mTorr). Second, there is a curved portion commencing at approximately 75 mTorr and extending downward to the $CO_2$ base pressure of 30 mTorr. We defer the interpretation of this curvature to Sec. V, but pause here only to note that this feature has not been observed by the authors,[4] who have investigated $CO_2$ pressure broadening using saturation techniques. Observations similar to ours have been reported by Bagaev *et al.*[5] in methane.

In addition to the above collision partners, broadening data have been obtained on the 10.6-$\mu$m $P(20)$ transition for $CO_2$ perturbed by $^3He$, Ne, Ar, Kr, NO, CO, $O_2$, $NH_3$, and $CH_4$. Measurements have also been made on the $CO_2$ rotational-vibrational transitions 10.6-$\mu$m $P(12)$, $P(32)$, and $R(20)$, and 9.6-$\mu$m $P(20)$ for $CO_2$ in collision with $CO_2$, $N_2$,

$H_2$, $D_2$, $^4He$, and Xe. The results of these measurements, with proper adjustment for saturation effects, will be presented in Sec. V.

Figure 6 depicts the intensity dependence of the FWHM of the saturated resonance as a function of pressure in pure $CO_2$ for three different laser intensities. The peak intensity in the internal absorption cell is calculated with the formula

$$I = 2P/\pi w^2(1-R), \tag{1}$$

where $P$ is the ouput power of the probe oscillator, $w$ is the mode radius[6] in the cell, and $R$ is the reflectivity of the output mirror. With a mirror reflectivity of 98%, a mode radius of 0.35 cm, the intracavity intensities for the three output powers of 0.220, 0.147, and 0.073 W are, respectively, 55, 37, and 18 W/cm$^2$.

## IV. THEORY OF $CO_2$ 4.3-$\mu$m SATURATION RESONANCE

The standing-wave tuning dip in the output of an atomic laser was first predicted by Lamb[7] for low laser intensities. Recently several high intensity theories have been advanced.[8-10] The effects of collisions on the line shapes of atomic laser systems have also received considerable attention.[11-16] A treatment of the Lamb-dip formation in a molecular system (CO) was recently given by one of us (H.A.H.).[17]

Although theoretical descriptions of the standing-wave saturation resonance in an absorbing medium have been developed,[2,18] there is no comprehensive theoretical treatment that includes the effects of both weak and strong collisions and saturation broadening, yet is simple enough to permit curve matching to experimental results. For this reason we have developed an approximate theory which permits a closed-form solution. We disregard the effect upon the line shape of weak collisions which change the particle velocities by a small amount. The homogeneous portion of the linewidth is then determined by $\Delta\nu_L = 1/\pi T_2$, where $T_2$ is the dephasing[19] time ($\Gamma$ of Ref. 19). This assumption has been shown to be valid at relatively high pressures, when the angle change of the velocities due to a weak collision $\theta$ satisfies the inequality $\Delta\omega_D\theta > 1/T_2$, where $\Delta\omega_D$ is the Doppler linewidth. Under this assumption, it is possible to obtain rate equations for the diagonal elements of the density matrix. The rate equations permit solutions that are not limited to third-order perturbation theory, and thus contain the effects of saturation broadening, important in the experiments reported here.

The "strong" collisions redistribute the "local" hole (in velocity space) of the population inversion among the velocity groups; this redistribution is termed cross relaxation and is described by a convolution integral with the collision kernal $\Gamma(v, v')$. Inelastic collisions also produce rotational state changes; these occur at the rate $\gamma$. The inverse of $\gamma$ is $T_1$. $V$-$V$, $V$-$T$, and $V$-$R$ processes are ignored.

We formulate our theory of the saturation resonance in the $CO_2$ 4.3-$\mu$m fluorescence in terms of a two-level system where the upper level (2) is a given rotational state ($J$) of the $CO_2$ $|00^01\rangle$ vibrational level and the lower level (1) is the appropriate rotational state ($J \pm 1$) of either the $|10^00\rangle$ or $|02^00\rangle$ vibrational level. The following equation holds for the time rate of change of the population of the lower state ($n_1$) of the $CO_2$ absorber gas in the presence of a standing-wave $CO_2$ laser electric field, where $I$ is the intensity of one of the running wave components:

$$\frac{\partial n_1(v)}{\partial t} = -\gamma(v)n_1(v) - \int \Gamma(v', v)n_1(v)\,dv' + \int \Gamma(v, v')n_1(v')\,dv' + R_1(v) - \sum_k \sigma(v, k, \omega)[n_1(v) - n_2(v)]\frac{I}{\hbar\omega}. \tag{2}$$

The equation for the upper-state population ($n_2$) is

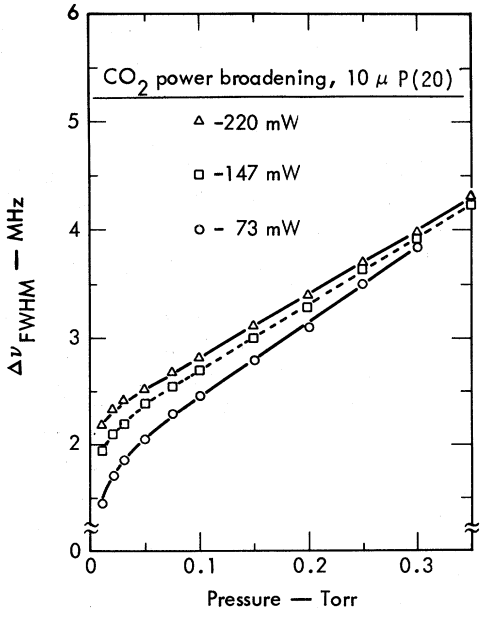


FIG. 6. $CO_2$ power-broadening data on the 10.6-$\mu$m $P(20)$ transiton for the three laser output powers of 0.220, 0.147, and 0.073 W.

$$\frac{\partial n_2(v)}{\partial t} = -\gamma(v)n_2(v) - \int \Gamma(v', v)n_2(v)\,dv' + \int \Gamma(v, v')n_2(v')\,dv' - \sum_k \sigma(v, k, \omega)[n_2(v) - n_1(v)]\frac{I}{\hbar\omega}. \quad (3)$$

The degeneracy factors $(g_1, g_2)$ of the upper and lower levels have been omitted in Eqs. (2) and (3), since $g_1/g_2 \approx 1$. In Eqs. (2) and (3), $\Gamma(v, v')$ and $\Gamma(v', v)$ are the cross-relaxation rates between the pairs of velocity groups $(v, v+dv)$ and $(v', v'+dv')$. We assume that they are equal for the upper and lower levels. $R_1$ of Eq. (2) is a pump term; we assume that the upper level (2) is not pumped ($R_2 = 0$). Finally, $\sigma(v, k, \omega)$ is the optical cross section for induced transitions within the velocity group $v, v+dv$, at frequency $\omega$ and wave vector $k$, while $\gamma$ represents relaxation rates to levels other than those considered.

The equilibrium densities of the two levels $n_1^e(v)$ and $n_2^e(v)$ have the same Maxwellian distribution of velocities $f_e(v)$:

$$n_1^e(v) \propto f_e(v), \quad n_2^e(v) \propto f_e(v), \quad (4)$$

where

$$f_e(v) = [1/(\pi\Delta v)^{1/2}]e^{-v^2/2(\Delta v)^2} \quad (5)$$

properly normalized such that

$$\int f_e(v)\,dv = 1.$$

The root-mean-square width of the Gaussian, Eq. (5), is

$$\Delta v = (kT/m)^{1/2}.$$

The steady-state solutions of Eqs. (2) and (3) are obtained by setting the time derivatives equal to zero. The resulting equations can be solved if we first make some assumptions concerning the relaxation rates $\gamma$ and $\Gamma$. First, we assume that $\gamma$ is independent of $v$. Next, using the principle of detailed balance we write

$$\Gamma(v, v')f_e(v') = \Gamma(v', v)f_e(v). \quad (6)$$

We also assume that the cross relaxation rate $\Gamma$ is independent of velocity[20]

$$\Gamma(v, v')f_e(v') = (1/\tau)f_e(v)f_e(v'), \quad (7)$$

where $\tau$ is a measure of the cross-relaxation time. Finally, we set

$$R_1(v) = Rf_e(v). \quad (8)$$

Incorporating the postulates (6)–(8) into Eqs. (2) and (3), we may derive the following equation for the steady-state population sums:

$$-\gamma[n_1(v)+n_2(v)] - \frac{1}{\tau}\int f_e(v')[n_1(v)+n_2(v)]\,dv' + \frac{1}{\tau}\int f_e(v)[n_1(v')+n_2(v')]\,dv' + Rf_e(v) = 0. \quad (9)$$

A solution of (9) is clearly

$$n_1(v) + n_2(v) = (R/\gamma)f_e(v). \quad (10)$$

Equation (10) states that the sum population is proportional to the ratio of the pump term to the decay rate to other levels. Note that there is no dependence on the induced transition term, and that cross relaxation $(1/\tau)$ is not involved in this result.

Next we form the steady-state population difference $\Delta n(v) = n_2(v) - n_1(v)$ by subtracting Eq. (3) from Eq. (2) and using our above assumptions:

$$-\gamma\Delta n(v) - \frac{\Delta n(v)}{\tau} + \frac{f_e(v)}{\tau}\int \Delta n(v')\,dv' - Rf_e(v) - \frac{2I\sigma_0}{\hbar\omega}W(v)\Delta n = 0. \quad (11)$$

In Eq. (11), $\sigma_0$ is the cross section on resonance

$$\sigma_0 = \lambda^2 T_2/4\pi\tau_{\text{spon}}, \quad (12)$$

and $W(v)$ is defined to be

$$W(v) = \frac{1}{\sigma_0}\sum_k \sigma(v, k, \omega). \quad (13)$$

A solution for the population difference $\Delta n(v)$ in Eq. (11) is

$$\Delta n(v) = A[1 + BW(v)]^{-1}f_e(v), \quad (14)$$

where $A$ and $B$ are constants to be determined by substituting (14) into (11) and equating functional dependences on $v$. The solution (14) implies local hole burning in the velocity range within which the optical cross-section function $W(v)$ differs from zero. Also, (14) contains saturation broadening of the hole because $W(v)$ appears in the denominator; when $BW(v)$ becomes larger than unity at the center of the hole, the "wings" of the hole are enhanced compared with the center. Proceeding with the substitution we find

$$-\left(\gamma + \frac{1}{\tau}\right) - AR - \frac{2I\sigma_0 W}{\hbar\omega} + \frac{1}{\tau}F(B) - ABWR + \frac{BW}{\tau}F(B) = 0, \quad (15)$$

where we have defined the function of $B$, $F(B)$, to be

$$F(B)=\int \frac{f_e(v')\,dv'}{1+BW(v')}. \tag{16}$$

By equating the coefficients of the powers of $W$ in Eq. (15) to zero we obtain the following expressions for the constants $A$ and $B$:

$$A=-\frac{1}{R}\left[\left(\gamma+\frac{1}{\tau}\right)-\frac{1}{\tau}F(B)\right] \tag{17}$$

and

$$B=2I\sigma_0/\hbar\omega(\gamma+1/\tau). \tag{18}$$

Note that $B$ in Eq. (18) does not depend on the function $F(B)$. Note also that the functional dependence of $F(B)$, in addition to the variables explicitly defined in Eq. (18), is on the frequency separation between the two signals [since

$$\sum_k \sigma(\omega, v, k)$$

depends on it] and on the homogeneous linewidth of the medium.

Substituting Eq. (17) into Eq. (14) we may write $\Delta n$ as

$$\Delta n=-\frac{R}{[1/T_1^*-F(B)/\tau](1+WB)}f_e, \tag{19}$$

where we have defined $1/T_1^*=\gamma+1/\tau$ as the sum of rotational plus cross-relaxation rates.

The population of the upper state $n_2$ is seen to be

$$n_2=\tfrac{1}{2}[(n_1+n_2)+\Delta n]. \tag{20}$$

Substituting Eqs. (10) and (19) in Eq. (20) yields

$$n_2=\frac{R}{2}\left(\frac{1}{\gamma}-\frac{1}{[1/T_1^*-F(B)/\tau](1+WB)}\right)f_e. \tag{21}$$

In the experiment the fluorescence from the upper ($00^01$) state to the ground ($00^00$) state is observed. This is obtained by integrating Eq. (21) over velocity

$$\int n_2(v)\,dv=\frac{R}{2}\left(\frac{1}{\gamma}-\frac{F(B)}{[1/T_1^*-F(B)/\tau]}\right). \tag{22}$$

We have developed a computational program (SINGL) which numerically evaluates the saturated resonance line shape Eq. (22) as a function of frequency. Typical results for the fluorescence line shape appear in Fig. 7. The dotted curve in this figure is a Lorentzian which has the same FWHM as the SINGL calculation, and it is evident that the theoretical line shape is very nearly Lorentzian. This result substantiates our use of a Lorentzian parametrization in reducing the data obtained in Sec. III.

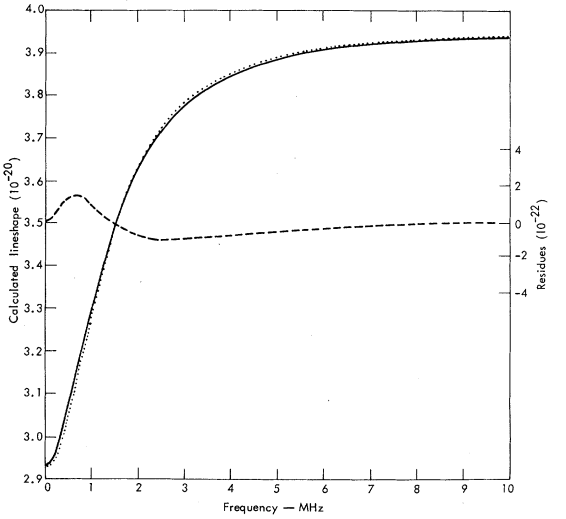


FIG. 7. Numerical solution of the saturated resonance line shape (solid line) and a Lorentzian (dotted line) with the same FWHM. Residues (dashed line) are shown against the right-hand ordinate.

## V. COMPARISON BETWEEN THEORY AND EXPERIMENT

The theoretical dependence of the FWHM of the resonance fluorescence calculated by SINGL as a function of pressure and intensity is demonstrated by the dotted curves in Fig. 8. These results follow the behavior normally expected for the FWHM ($\Delta\nu$) of a power-broadened homogeneous line which is given by the expression

$$\Delta\nu=\Delta\nu_L(1+I/I_s)^{1/2}, \tag{23}$$

where $I_s$ is the saturation intensity [$=(hc/8\pi)\mu^2T_1T_2$]. Comparing these results with out experimental data (Fig. 4) we observe that the theory does not accurately represent the low-pressure behavior of the FWHM data.

There are two possible explanations for the discrepancy. The point of view adopted by Alekseev *et al.*[19] is that the slope increase at low pressures is due to the emergence of the weak-collision contribution to the linewidth, which takes place at low pressures. They show theoretical curves which go to zero at zero pressure, because their analysis does not include the effect of saturation broadening or the finite spatial extent of the beam. There is another possible explanation of the discrepancy, owing to the finite transit time of the particles in the optical beam. We elaborate further on this mechanism to draw attention to its importance in those experiments which attempt to extract information on the cross sections of weak and strong collisions from the ratio of slopes of experimental

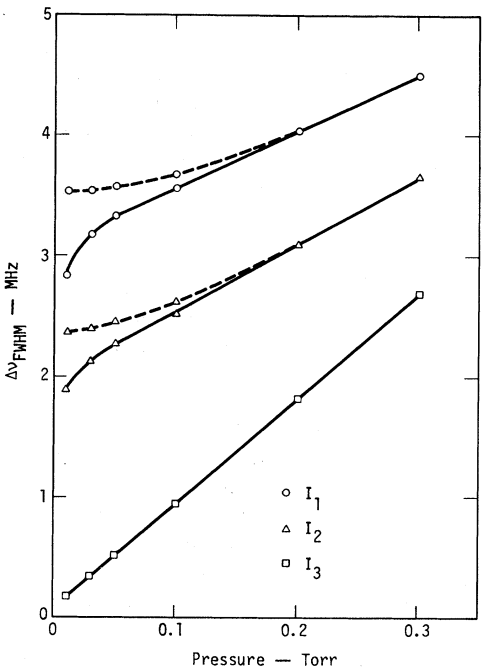


FIG. 8. Intensity dependence of the theoretical FWHM vs pressure for three different saturation intensities. For the dotted curves no transit time is considered; for the solid curves a phenomenological transit time is added to the theory. The intensities are such that $I_1 > I_2 > I_3$.

curves such as the one of Fig. 4.

The transit-time effect can be taken into account by adding a phenomenological inverse transit time $(1/T_0)$ to the relaxation terms $1/T_1$ and $1/T_2$ of the theory in Sec. IV. We find that we can accurately match both the high- and low-pressure dependence of the data as illustrated by the solid curves in Fig. 8. The value of the time-of-flight linewidth necessary to achieve this correspondence is approximately 59 kHz ($T_0 = 5.4 \times 10^{-6}$ sec). An estimate of the time-of-flight linewidth has been obtained by Hall[2] using a Fourier analysis of the optical pulse the molecule experiences in transiting the beam; the result is

$$\Delta\nu = 0.375\bar{v}/w, \tag{24}$$

where $\bar{v}$ is the mean molecular velocity and $w$ the mode radius. For $CO_2$ in a mode of radius 35 mm, $\Delta\nu \approx 43$ kHz. This is in reasonable agreement with our value of 59 kHz.

The changed behavior of the curves can be understood qualitatively from (23). Introducing the explicit dependences upon $T_1$ and $T_2$ in (23) one has

$$\Delta\nu = \left[\left(\frac{1}{\pi T_2}\right)^2 + \frac{T_1}{T_2}\left(\frac{\mu E}{\hbar}\right)^2\right]^{1/2}. \tag{25}$$

If $T_1 > T_2$, and if a transit-time contribution $1/T_0$ independent of pressure is added to both $1/T_1$ and $1/T_2$, then with decreasing pressure, $1/T_1$ reaches a pressure-independent value before $1/T_2$. The second term in (25) starts decreasing with decreasing pressure, rather than remaining pressure independent, causing a lowering of the extrapolated zero-pressure intercept.

The addition of the transit time to the theory provides the correct qualitative description of our data, yet we find that if reasonable values of $T_1^*$ and $T_2$ are used the theoretical intensity required to fit the experimental data is roughly a factor of three lower than the experimentally measured intensity. This problem is readily corrected by noting that the theory considers only a single intensity while in the actual experiment the fluorescence observed by the detector is the summation of the light emitted by axially symmetric volume elements of the $CO_2$ absorber gas which are subjected to the Gaussian intensity distribution

$$I = I_0 e^{-2r^2/w^2}. \tag{26}$$

With this in mind, our program was modified to solve for the shape of the fluorescence resonance in each a series of 0.05-mm-thick (radially) annular rings in which the intensity falls off according to the above prescription. The line shape found in each ring is weighted by the ratio of the area of the ring to the total beam area; then all the line shapes are summed and the FWHM of the resulting sum line shape is determined. Using this technique and appropriate values of $T_1^*$, we obtain an adequate correlation of the observed intensity in the high-pressure linear region.

Using our theoretical program, we proceed first with the reduction of the $CO_2$-$CO_2$ power-broadening data (Fig. 6) by varying the values of $T_1^*$ and $T_2$ to match the experimental data points for the three observed intensities of 55, 37, and 18 W/cm$^2$. The results of these calculations appear in Table I. We also list in this table the values of $T_1^*$ and $T_2$ necessary to fit a set of $CO_2$-$CO_2$ data taken on the same transition in an external absorption cell with an intensity of 11 W/cm$^2$. The power-corrected 10.6-$\mu$m $P(20)$ $CO_2$ self-broadening coefficient of 8.5 MHz/Torr seems to be very consistent over the three ranges of intensity for the internal cell power-broadening data and for the external cell data. This power-corrected value is ~20% larger than the uncorrected value of 7.1 MHz/Torr obtained directly from the slope of the experimental curve. The variation of $1/\pi T_1^*$ with intensity in Table I shows that this parameter is less accurately determined by the curve-matching procedure. Our average value of 3.4 MHz/Torr for this quantity lies between the value of 5 MHz/Torr de-

TABLE I. Calculated values of $I$, $T_1^*$, and $T_2$ including $CO_2$ power broadening.

| Intensity ($W/cm^2$) | $1/\pi T_1^*$ (MHz/Torr) | $1/\pi T_2$ (MHz/Torr) |
|---|---|---|
| | Internal absorption cell | |
| 55 | 4.0 | 8.5 |
| 37 | 3.5 | 8.5 |
| 18 | 2.5 | 8.5 |
| | External absorption cell | |
| 11 | 3.4 | 8.5 |

termined by Granek[21] for $1/\pi T_1^*$ and a recent determination[22] of the $CO_2$-$CO_2$ rotational relaxation ($1/\pi T_1$) value of 2.4 MHz/Torr.

The experimentally determined pressure-broadening data of Sec. III can now be corrected for the influence of saturation and the broadening coefficients obtained by fitting the data points for each perturber with the theoretical line-shape program. There are three independent variables to be determined: $I$, $T_1^*$, and $T_2$. We proceed by using the above value of $T_1^*$ for $CO_2$ and varying $I$ and $T_2$ to fit the $CO_2$ self-broadening data points. Next, the $CO_2$-perturber data may be reduced by keeping the intensity found for the $CO_2$ self-broadening data fixed and varying $T_1^*$ and $T_2$ in the theoretical program to fit the perturber data. The broadening coefficients obtained in this manner are listed in Tables II and III. In all of these calculations the spontaneous lifetime used was 5 sec as determined by a recent measurement.[23]

## VI. COMPARISON OF POWER-CORRECTED LINE-BROADENING COEFFICIENTS WITH OTHER DETERMINATIONS

Other recent determinations[23-32] of the self-broadened linewidth of $CO_2$, or the linewidth of $CO_2$ broadened with foreign gases, have been made primarily using a $CO_2$ laser absorption technique which was first described in 1966 by McCubbin *et al.*[24] and Gerry and Leonard.[25] Using this method, the rotational dependence of the $CO_2$ and $CO_2$-$N_2$ linewidths have also been investigated. Measurements of the effects of other foreign gases on the $CO_2$ linewidth are sparse and are limited to $CO_2$-He, $CO_2$-CO, $CO_2$-Ar, and $CO_2$-$O_2$. In general, these authors present their results in a variety of terminology, the most popular of which

TABLE II. Power-corrected $CO_2$ pressure-broadening coefficients for the 10.6-$\mu$m $P(20)$ transition.

| Collision partner | Broadening coefficient (MHz/Torr) | Cross section ($\sigma$) $cm^2(10^{-14})$ | Absorption line half-width ($\gamma_{1/2}$) ($cm^{-1}\,Atm^{-1}$) |
|---|---|---|---|
| $CO_2$ | 8.5 ± 0.4 | 1.57 ± 0.08 | 0.108 ± 0.005 |
| $N_2O$ | 9.1 ± 0.5 | 1.68 ± 0.08 | 0.115 ± 0.006 |
| $N_2$ | 7.4 ± 0.4 | 1.20 ± 0.06 | 0.094 ± 0.005 |
| NO | 7.0 ± 0.4 | 1.16 ± 0.06 | 0.089 ± 0.005 |
| CO | 6.5 ± 0.3 | 1.06 ± 0.05 | 0.082 ± 0.004 |
| $O_2$ | 5.6 ± 0.3 | 0.95 ± 0.05 | 0.071 ± 0.004 |
| $H_2$ | 13.7 ± 0.7 | 0.74 ± 0.04 | 0.174 ± 0.009 |
| $D_2$ | 9.5 ± 0.5 | 0.72 ± 0.04 | 0.120 ± 0.006 |
| $^3He$ | 5.7 ± 0.3 | 0.37 ± 0.02 | 0.072 ± 0.004 |
| $^4He$ | 5.4 ± 0.3 | 0.41 ± 0.04 | 0.068 ± 0.004 |
| Ne | 5.0 ± 0.3 | 0.73 ± 0.04 | 0.063 ± 0.004 |
| Ar | 5.0 ± 0.3 | 0.90 ± 0.05 | 0.063 ± 0.004 |
| Kr | 5.1 ± 0.3 | 1.08 ± 0.05 | 0.065 ± 0.004 |
| Xe | 6.7 ± 0.3 | 1.51 ± 0.08 | 0.085 ± 0.004 |
| $NH_3$ | 11.1 ± 1.0 | 1.53 ± 0.14 | 0.141 ± 0.013 |
| $CH_4$ | 11.0 ± 0.6 | 1.48 ± 0.07 | 0.139 ± 0.007 |

TABLE III. Power-corrected $CO_2$ pressure-broadening coefficients for various transitions.

| Transition | Collision partner | Broadening coefficient (MHz/Torr) | Cross section ($\sigma$) $cm^2(10^{-14})$ | Absorption line half-width ($\gamma_{1/2}$) ($cm^{-1}$ $Atm^{-1}$) |
|---|---|---|---|---|
| 10.6 $\mu$m | $CO_2$ | 8.4 ± 0.4 | 1.55 ± 0.08 | 0.106 ± 0.005 |
| $P(12)$ | $N_2$ | 7.3 ± 0.4 | 1.10 ± 0.06 | 0.093 ± 0.005 |
| | $H_2$ | 13.7 ± 0.7 | 0.74 ± 0.04 | 0.174 ± 0.009 |
| | $D_2$ | 9.8 ± 0.5 | 0.74 ± 0.04 | 0.124 ± 0.006 |
| | $^4He$ | 4.9 ± 0.3 | 0.37 ± 0.02 | 0.062 ± 0.004 |
| | Xe | 6.3 ± 0.3 | 1.42 ± 0.07 | 0.080 ± 0.004 |
| 10.6 $\mu$m | $CO_2$ | 8.8 ± 0.4 | 1.62 ± 0.08 | 0.112 ± 0.006 |
| $P(32)$ | $N_2$ | 7.4 ± 0.4 | 1.20 ± 0.06 | 0.094 ± 0.005 |
| | $H_2$ | 13.2 ± 0.7 | 0.72 ± 0.04 | 0.167 ± 0.008 |
| | $D_2$ | 9.8 ± 0.5 | 0.74 ± 0.04 | 0.124 ± 0.006 |
| | $^4He$ | 5.7 ± 0.3 | 0.43 ± 0.02 | 0.072 ± 0.004 |
| | Xe | 6.5 ± 0.3 | 1.47 ± 0.07 | 0.082 ± 0.004 |
| 10.6 $\mu$m | $CO_2$ | 8.5 ± 0.4 | 1.57 ± 0.08 | 0.108 ± 0.005 |
| $R(20)$ | $N_2$ | 6.5 ± 0.3 | 1.06 ± 0.05 | 0.082 ± 0.004 |
| | $H_2$ | 13.2 ± 0.7 | 0.72 ± 0.04 | 0.167 ± 0.008 |
| | $D_2$ | 9.5 ± 0.5 | 0.72 ± 0.04 | 0.120 ± 0.006 |
| | $^4He$ | 4.9 ± 0.3 | 0.37 ± 0.02 | 0.062 ± 0.004 |
| | Xe | 6.3 ± 0.3 | 1.42 ± 0.07 | 0.080 ± 0.004 |
| 9.6 $\mu$m | $CO_2$ | 10.7 ± 0.5 | 1.97 ± 0.10 | 0.135 ± 0.007 |
| $P(20)$ | $N_2$ | 8.3 ± 0.4 | 1.35 ± 0.07 | 0.105 ± 0.005 |
| | $H_2$ | 14.0 ± 0.7 | 0.76 ± 0.04 | 0.177 ± 0.009 |
| | $D_2$ | 12.0 ± 0.6 | 0.90 ± 0.04 | 0.152 ± 0.008 |
| | $^4He$ | 6.2 ± 0.3 | 0.47 ± 0.02 | 0.078 ± 0.004 |
| | Xe | 8.1 ± 0.4 | 1.83 ± 0.09 | 0.103 ± 0.005 |

seem to be (i) absorption line half-width $\gamma_{1/2}$ ($cm^{-1}$ $atm^{-1}$) and (ii) optical cross section $\sigma$ ($cm^2$). We have tabulated some of their representative values in Table IV. We have also changed our measurements of $1/\pi T_2$ (Tables II and III) to these two conventions using the following conversions:

(i) $1/\pi T_2$ (MHz/Torr) to absorption line half-width ($cm^{-1}atm^{-1}$)

$$\gamma_{1/2}=\frac{1/\pi T_2\ (\text{MHz/Torr})\times 760\ (\text{Torr/atm})}{2\times c\ (\text{cm/sec})}; \quad (27)$$

(ii) $1/\pi T_2$ (MHz/Torr) to optical cross section ($cm^2$)

$$\sigma=\frac{1/\pi T_2\ (\text{MHz/Torr})}{n\ (\#/\text{cm}^3\,\text{Torr})\times \bar{v}\ (\text{cm/sec})}, \quad (28)$$

where

$$\bar{v}=(8kT/\pi\mu)^{1/2} \text{ and } n=3.25\times 10^{16}\,\text{cm}^{-3}\,\text{Torr}^{-1},$$

with $\mu$ representing the appropriate reduced mass. The only measurements of the $CO_2$ broadening coefficient which involve a direct determination of the homogeneous linewidth using saturation techniques similar to the procedure reported herein are those of Freed and Javan as well as some unpublished work by Feldman and Peterson.[4] No rotational investigations were made by these authors, and only $CO_2$ self-broadening was measured. Their results for the 10.6-$\mu$m $P(20)$ line are, respectively, 7.6, 8, and ~7 MHz/Torr. These values are somewhat lower than our power-corrected value of 8.5 MHz/Torr.

It is evident from Table IV that a comparison of our pressure-broadening results with those of oth-

TABLE IV. Published pressure-broadening data for the 9- and 10-$\mu$m bands of $CO_2$.

| Transition | Collision partners | Line half-width ($cm^{-1}$ $atm^{-1}$) Ref. 32 | Ref. 33 | Ref. 36 | Ref. 37 | Ref. 38 | Ref. 39 | Cross section ($10^{-14}$ $cm^2$) Ref. 30 | Ref. 27 | Ref. 41 |
|---|---|---|---|---|---|---|---|---|---|---|
| | $CO_2$-$CO_2$ | 0.096 | 0.096 | 0.093 | 0.099 | ~0.099 | 0.105 | 0.57 | 1.31 | 1.30 |
| | $CO_2$-$H_2$ | | 0.070 | | | 0.068 | | 0.5 | 1.14 | 0.87 |
| | $CO_2$-$O_2$ | | | | | | | | | 0.84 |
| 10.6-$\mu$m $P(20)$ | $CO_2$-$CO_2$ | | | | | | | 0.56 | | |
| | $CO_2$-He | | | | | | | 0.177 | 0.48 | 0.37 |
| | $CO_2$-Ar | | 0.077 | | | | | | | |
| 10.6-$\mu$m $R(20)$ | $CO_2$-$CO_2$ | | ~0.08 | ~0.093 | ~0.090 | | 0.108 | | | |
| 10.6-$\mu$m $P(12)$ | $CO_2$-$CO_2$ | | 0.105 | ~0.105 | ~0.11 | ~0.102 | 0.113 | | | |
| | $CO_2$-$N_2$ | | | | | ~0.070 | | | | |
| 10.6-$\mu$m $P(32)$ | $CO_2$-$CO_2$ | | | ~0.065 | ~0.091 | ~0.097 | 0.097 | | | |
| | $CO_2$-$N_2$ | | | | | ~0.086 | | | | |
| 9.6-$\mu$m $P(20)$ | $CO_2$-$CO_2$ | | 0.063 | | ~0.076 | | | | 1.36 | |

er authors is limited owing to the small number of perturbers which they have investigated. Where comparison is possible, we find that our power-corrected results on the 10.6-$\mu$m $P(20)$ transition are approximately 10% higher for $CO_2$ and as much as 30% higher for $CO_2$-$N_2$. The best agreement is found with the 10.6-$\mu$m $CO_2$ absorption work of Arié *et al.*[31] Their value of 0.105 $cm^{-1}$ $atm^{-1}$ for the $P(20)$ transition converts to 8.3 MHz/Torr; this is in excellent agreement with our value of 8.5 MHz/Torr. For the 9.6-$\mu$m $P(20)$ transition the disparity is, in general worse, with our values for $CO_2$ ranging from 30 to 70% higher than other published results. Another difference is that our data (Table III) reflect practically no rotational dependence for the 10.6-$\mu$m band, while the values obtained by others and displayed in Table IV indicate a small and monotonic decline of the broadening coefficient from low to high angular momentum quantum number $J$.[33]

The resolution of the question of rotational dependence using our technique appears to hinge on a correct evaluation of the rotational dependence of the effective dipole moment ($|\mu_z|^2$) in the presence of saturation. The main difference between our measurement and other determinations of the rotational quantum number dependence of the broadening coefficients is the influence of saturation. This is apparent from Eqs. (12) and (18) since the experimental intensity was the same for the $P(12)$, $P(20)$, and $P(32)$ data, and we assume that $T_1^*$ is independent of $J$.[34] A straightforward summation[35] of the dipole moment (in the absence of saturation) over the $m$ degenerate states for $P(12)$, $P(20)$, and $P(32)$ shows that the dipole moment changes a maximum of 4% between these transition. This estimate is substantiated by the experimentally determined variation of the dipole moment with $J$ found by Arie.[31] Saturation may alter this picture, however, since the saturating optical field will generate nonequilibrium populations of the $m$ levels producing a partial alignment of the system. The degree of alignment is determined by the balance of the induced radiative transitions against those of collisional reorientation. This complicated dynamical behavior modifies the coupling of the radiative field to the molecular systems and influences the saturated response of the medium.[36] The recent work of Goldreich *et al.*[37-39] on interstellar masers may provide a suitable starting point for investigating the effects of saturation involving degenerate levels.

We conclude this section by mentioning the correlation between our results and the work of Alcock of the Canadian Research Council. Alcock[40] is investigating high-pressure (1–15-atm) $CO_2$ amplifier systems and has measured the gain of the 9.6-$\mu$m $P(20)$ transitions as a function of pressure. Alcock has developed a theoretical model for the gain of these high-pressure $CO_2$ systems which includes the effect of line overlap. Using our pressure-broadening coefficients for $CO_2$, $N_2$, and He in this model, he calculates gain values which provide the best agreement with his data over the range 1–8 atm as compared to the broadening coefficients of other authors.[41] In particular, the experimentally observed fact that 9.6-$\mu$m gain becomes comparable to the 10.6-$\mu$m gain at high pressure is accurately predicted by this model using our broadening coefficients.

## VII. CALCULATION OF LINEWIDTHS USING MURPHY BOGGS THEORY

One of the major applications of the $CO_2$ pressure-broadening data obtained from these lineshape studies is the analysis of the dynamics of intermolecular collisions with the primary objective of characterizing the intermolecular forces involved in these collisions. The manner in which this is normally accomplished is to formulate a classical, semiclassical, or entirely quantum-mechanical description of the scattering problem taking into account the various intermolecular forces, and then, with certain approximations, determine the intensity distribution of the radiation absorbed (or emitted) on a given transition by the system which is undergoing such collisions. By correlating the results of these calculations with experimentally observed linewidths one may parametrize the magnitude of the various intermolecular forces.

The number and variety of pressure broadening theories available for this task is legion.[42] The formulation which has enjoyed the most successful and widespread application, however, is the Anderson-Tsao-Curnutte[43] (ATC) pressure-broadening theory. Another theory which has been successfully applied to microwave linebreadth data is that of Murphy and Boggs[44-47] (MB). We chose the MB treatment since they had obtained quadrupole moments for several of the perturbers ($CO_2$, $N_2O$, $N_2$, NO, $H_2$, and $D_2$) which we have investigated and had constructed a formalism which was readily adaptable for the analysis of our data.

The perturbers which we have investigated represent quadrupole-dipole, quadrupole-quadrupole, dispersion, and exchange interactions.[48] For most of the collision partners, with the exception of the rare gases, the longest-range interactions are quadrupole-dipole ($r^{-4}$) and quadrupole-quadrupole ($r^{-5}$). In the case of the $CO_2$-rare-gas interactions, the only potentials which are of consequence are dispersion and exchange forces. Two other perturbers rate special comment. Oxygen is unusual in that its ground state is $^3\Sigma_g^-$, and consequently has a magnetic dipole moment. NO is also unusual in that its ground state contains an unpaired electron in a $\pi$ orbital, and thus, a component of electronic angular momentum exists about its internuclear axis generating a magnetic moment. In this latter case, two fine-structure states, the $^2\Pi_{1/2}$ and the $^2\Pi_{3/2}$, are populated at room temperature. These systems involve additional magnetic interactions.

Boggs has been kind enough to provide us with a program which calculates the linewidths for prescribed collision partners using the MB theory. Unfortunately, $CO_2$–rare-gas collisions, could not be treated by this program, since exchange forces are not currently included in the theory. The perturbers $NH_3$ and $CH_4$ could also not be calculated. Before describing the results of calculations using this theory we wish to make a few qualitative remarks regarding the perturbers which could not be evaluated by the theory. One of the most striking points about the rare-gas perturbers is that they are all essentially equally effective (except for Xe and He) in broadening $CO_2$. Smith[49] points out that other broadening measurements performed with rare-gas perturbers result in linewidths which are higher for the low-mass (He) and high-mass (Xe) perturbers and lower for the intermediate-mass perturbers. The minimum of a plot of linewidth versus the mass of the rare gas occurs around the mass of the molecule which is being perturbed. A plot for our $CO_2$–rare-gas data is illustrated in Fig. 9, and is observed to demonstrate this trend. Although the minimum is fairly shallow, it is in the general neighborhood of the $CO_2$ mass (44). We note that the influence of velocity changing collisions is expected to become significant for perturber masses comparable to, and greater than, the mass of the radiator. The onset of this effect is approximately at the minimum observed in the data of Fig. 9. Rare-gas broadening has been calculated in the rotational spectrum of HCl by Krishnaji and Srivastava,[50] and by Gordon[51] using dispersion and exchange interactions. Recently, Tipping and Herman[52,53] and Boulet *et al.*[54] have considered the effects of vibration on HCl–rare-gas collisions and have achieved moderate agreement with the experimental data.

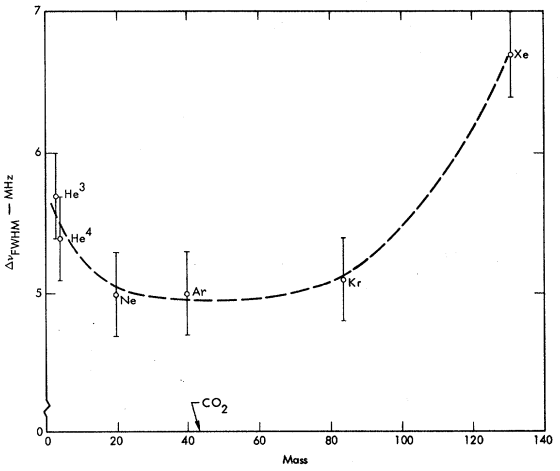


FIG. 9. Mass dependence of the $CO_2$ linewidth for various collision partners.

Two other interesting perturbers which we have investigated are $NH_3$ and $CH_4$. Both broaden $CO_2$ roughly the same amount (~11 MHz/Torr); only $H_2$ is more effective in broadening $CO_2$ in our data, presumably on account of its high velocity. The effectiveness of $NH_3$ in broadening $CO_2$ arises naturally as it has a large static dipole moment (0.847 D), although its quadrupole moment of ~2D Å is fairly small. Thus, the strong long-range dipole-quadrupole interaction between $NH_3$ and $CO_2$ would appear to account for the large measured broadening coefficient of these collision partners. The case of $CH_4$ is not so simple. Since it is a spherical top molecule with tetrahedral symmetry, $CH_4$ has no static dipole or quadrupole moment. In the absence of vibrations, it should appear similar to Ne (mass 20 vs a mass of 16 for $CH_4$) in perturbing $CO_2$. This is obviously not the case since the $CO_2$-$CH_4$ broadening coefficient is approximately 70% larger than that for $CO_2$-Ne. Vibrational effects may be the key here, especially the possibility of vibrational resonance since the $\nu_4$ mode of $CH_4$ at 1306.2 $cm^{-1}$ is well within $kT$ of the $CO_2$ $10^00$ level. Such effects, however, have not been investigated within the framework of existing broadening theories. However, it should be noted that octupolar interactions may also be important for the case of methane.

We turn now to a discussion of the results of linewidth calculations obtained with the Murphy-Boggs formulation. The molecular parameters used in the calculations appear in Table V, and the theoretical quadrupole moments required to fit our line broadening results are presented in Table VI. The only other linewidth calculations which have been made in the infrared for $CO_2$-$CO_2$ and $CO_2$-$N_2$ were done by Yamamoto *et al.*[55] and Boulet *et al.*[56] using the ATC theory. The results of Boulet are particularly interesting, since he is basing his calculation on the experimental $CO_2$ laser absorption data of Arie *et al.*[31] We noted in Sec. VI that Arie's value for $CO_2$ self-broadening on the 10.6-$\mu$m $P(20)$ line was in good correlation with our data (8.3 MHz/Torr vs our 8.5 MHz/Torr). Boulet's somewhat lower value of 7.6 D Å for the $CO_2$ quadrupole moment, compared to our value of 8.4 D Å, is understandable owing to two basic differences between the Murphy-Boggs theory and the Anderson-Tsao-Curnette theory. First, the collisions in the ATC theory are somewhat "harder" than in the MB formulation, owing to a difference in the collision efficiency function. Second, since the MB theory was developed specifically for the microwave region, it considers only inelastic collisions. In the infrared, however, the contribution of elastic processes to the linewidth must be taken into consideration.

Boulet *et al.* also measured the $CO_2$-$N_2$ broadening coefficient and used the ATC theory to obtain the value of the $N_2$ quadrupole moment. However, since their value for the $CO_2$-$N_2$ broadening coefficient of 5.9 MHz/Torr on the 10.6-$\mu$m $P(20)$ transition is considerably smaller than our result (7.4 MHz/Torr), we would expect our calculation of the $N_2$ quadrupole moment to be substantially larger than their result. Our 7.3 D Å value for the $N_2$ quadrupole moment is almost twice the 3.7 D Å found by Boulet.

Comparing our determinations of the quadrupole moments tabulated in Table VI with the results of other investigations, we may make the following observations. For the 10.6-$\mu$m $P(20)$ data, our value for the $CO_2$ quadrupole moment seems to be in good agreement with most other results including the value suggested by Stogryn and Stogryn.[57] In particular, it agrees almost exactly with the microwave results calculated by Murphy and Boggs.[46] For $N_2O$, however, there is a large disparity with most other values except for nuclear spin relaxation. Our result is ~50% larger than the MB calculation. This discrepancy may be attributable to vibrational resonance, since both the $10^00$ and $00^01$ states of $CO_2$ and $N_2O$ are only ~100 $cm^{-1}$ apart.

Our $N_2$ quadrupole moment agrees with the MB result, but is almost a factor of two larger than most other determinations. The quadrupole moment for NO agrees exactly with the MB result, but is ~30% larger than other values. Murphy and Boggs did not make any calculations for CO or $O_2$. Our result for CO is in good agreement with the value suggested by Stogryn and Stogryn and with most other values. The quadrupole moment we calculate for $O_2$ is considerably larger than any other values. We find a similar problem with the $H_2$ and $D_2$ quadrupole moments. Even though we agree with the MB value, our calculation is ~2 or 3 times larger than any other determination.

A comparison of the broadening due to CO and $N_2$ and the resulting quadrupole moments obtained is instructive, since these molecules are isoelectronic and equal in mass. Although CO has a larger theoretically calculated quadrupole moment than $N_2$ (these calculations seem fairly well substantiated by both nuclear spin relaxation and second virial coefficient data) and a small dipole moment which is absent for $N_2$, CO is less effective in broadening $CO_2$ than $N_2$ by ~15%. Once again it appears that vibrational effects may play an important role here, since the first excited vibration of $N_2$ is only 10 $cm^{-1}$ above the $CO_2$ $00^01$ level.

The quadrupole moment for $O_2$ required to fit the data is 4.4 times as large as that suggested by Stogryn and Stogryn. One of the major reasons for

TABLE V. Physical constants of various collisional partners.

| Molecule | Molecular mass | Dipole moment $\mu$ (D) | Rotational constant $B_0$(GHz) | Ionization potential $\epsilon$ (eV) | Polarizability anisotrophy $(\alpha_{11}-\alpha_1)$ (Å$^3$) | Average polarizability $\bar{\alpha}$ (Å$^3$) |
|---|---|---|---|---|---|---|
| $N_2O$ | 44.015 03 | 0.166 | 12.566 166 | 12.9 | 2.79 | 3.00 |
| $N_2$ | 28.0134[b] | ••• | 60.3 | 15.51 | 0.93 | 1.76 |
| NO | 30.01[b] | 0.16 | 51.0845 | 9.5 | 1.05 | 1.64 |
| CO | 28.01[b] | 0.10[a] | 57.8975[a] | 14.01[b] | 0.975[c] | 1.95[c] |
| $H_2$ | 1.0080[b] | ••• | 1824.0 | 15.6 | 0.22 | 0.79 |
| $CO_2$ | 44.0088 | ••• | 11.8 | 14.4 | 2.10 | 2.65 |
| $D_2$ | 2.0160[b] | ••• | 912.87 | 15.6 | 0.22 | 0.79 |
| $O_2$ | 31.9988[b] | ••• | 43.102[a] | 12.06[b] | 1.14[c] | 1.6[c] |

Except where indicated, all values are from Table X of Ref. 46.

[a]Reference 35.
[b]Reference 61.
[c]Reference 62.

this is that it appears to be necessary to take into account the effects of exchange forces. Note that the $CO_2$-$O_2$ linewidths are not much larger than the $CO_2$-rare-gas values. Dillon and Godfrey[58] have made broadening calculations taking into account the influence of exchange forces and have obtained good agreement with $O_2$ microwave pressure-broadening data.

The $H_2$ and $D_2$ quadrupole moments are roughly a factor of 3 larger than the values suggested by Stogryn and Stogryn; the factors governing this difference are not clear, although vibrational effects and exchange terms may both play a role.

The fact that the MB theory provides reasonable quadrupole moments for only two of the perturbers which we have investigated ($CO_2$ and CO) is attributable to two factors: (i) since the MB theory was developed for the microwave regime, only inelastic collisions are considered; (ii) obviously no attempt was made by Murphy and Boggs to account for vibrational effects. It would appear that consistent with the historical determinations of mole-

TABLE VI. Results of various determinations of molecular quadrupole moments.

| | ($Q_{mol}$, in units of debye-angstroms) | | | | | | |
|---|---|---|---|---|---|---|---|
| Molecule | $Q_{mol}$; this work[q] 10-$\mu$m $P(20)$ | 9-$\mu$m $P(20)$ | $CO_2$ Laser absorption data | Microwave data[c] | Theoretical calculation | Second virial coefficient[o] | Nuclear spin relaxation[p] |
| $CO_2$ | 8.4±0.6 | 10.9±0.8 | 7.19,[a] 7.6[b] | 8.44±0.98 | 5.0,[d] 5.28[e] 8.6[f] | 8.2, 9.18 10.0, 11.6 | 9.70 |
| $N_2O$ | 9.3±1.5 | ••• | ••• | 6.07±0.42 | 7.40–7.50[g] 6.0[f] | 5.56 | 8.50 |
| $N_2$ | 7.3±1.2 | 7.5±1.0 | 3.28,[a] 3.7[b] | 6.14±0.35 | 5.04,[h] 2.72[i] 3.04[f] | 4.1, 3.8 3.6 | 3.40 |
| NO | 6.1±1.4 | ••• | ••• | 6.07±0.42 | 1.76,[j] 3.6[f] | 4.4, 4.8 | 4.10 |
| CO | 5.1±0.8 | ••• | ••• | ••• | 4.40,[k] 3.62[l] 5.0[f] | 5.62 | 4.0 |
| $O_2$ | 3.4±0.7 | ••• | ••• | ••• | 1.18,[j] 2.06[m] 1.97,[p] 0.78[f] | 3.8 | 1.84 |
| $H_2$ | 4.5±0.6 | 3.6±0.5 | ••• | 3.37±1.23 | 1.324,[n] 1.298[f] | 1.20 | 1.04, 1.90 |
| $D_2$ | 3.1±0.3 | 4.0±0.3 | ••• | 3.37±1.23 | 1.296[f] | ••• | ••• |

[a]Reference 63.
[b]Reference 64.
[c]Calculated by Murphy and Boggs, Ref. 46.
[d]Reference 65.
[e]Reference 66.
[f]Recommended by Ref. 67.
[g]Reference 68.
[h]Reference 69.
[i]Reference 70 (see also, Ref. 71).
[j]Reference 67.
[k]Reference 72 (see also, Ref. 71).
[l]Reference 73.
[m]Reference 74.
[n]Reference 75.
[o]Data given by Refs. 46 and 67.
[p]Reference 76.
[q]Error bars reflect only errors in the data.

cular quadrupole moments through linewidth measurements that present theories do not provide a sensitive evaluation of these moments.

We also conclude from our results that it is apparent that the proper treatment of vibrational effects is essential to the ultimate understanding of line broadening in rotational-vibrational spectrum. Unfortunately, there is currently no theory which fully accounts for all the internal degrees of freedom that enter into the potential between two colliding molecules and results in a linewidth for a given rotational-vibrational transition. Oka[42] has recently described some of the problems which are involved in such theoretical description. The vibrational dependence of the intermolecular potential in collisions has been investigated,[59] but not simultaneously with the angular dependence. Recent semiempirical modifications have been made to the ATC theory in an attempt to describe rotational-vibrational data.[52-53,60]

## VIII. SUMMARY AND CONCLUSIONS

Using a high resolution infrared spectrometer comprised of stable $CO_2$ oscillators we have made accurate linebreadth measurements of the saturated resonance in the $CO_2$ 4.3-$\mu$m fluorescence as a function of pressure and intensity and for a wide variety of collision partners. Numerical reduction of the data using a Lorentzian profile to least-squares fit the the saturated line shape provides an excellent characterization of the observed line shape over the range of pressures investigated. Experimental pressure-broadening data have been obtained for $CO_2$ in collision with $CO_2$, $N_2$, $H_2$, $D_2$, $^4He$, and Xe on the 10.6-$\mu$m $P(12)$, $P(20)$, $P(32)$, and $R(20)$ transitions and on the 9.6-$\mu$m $R(20)$ line. In addition, data for the perturbers $^3He$, Ne, A, Kr, $N_2O$, $NH_3$, $CH_4$, NO, CO, and $O_2$ have been found for the 10.6-$\mu$m $P(20)$ transition.

A semiclassical theory of the 4.3-$\mu$m saturated resonance has been developed which accounts for the influence of $T_1^*$ (rotational plus cross relaxation), $T_2$ (phase interruption), and $I$ (intensity) on the line shape. To properly describe the low-pressure (0–75-mTorr) behavior of the data we find it necessary to add a phenomenological transit time ($T_0$) to $T_1^*$ and $T_2$ in our theory. The time-of-flight linewidth obtained in this manner is 59 kHz, which is in reasonable agreement with other estimates of this quantity. Our theory indicates that the low-pressure behavior due to the transit time is an intensity dependent effect. At high saturating intensities the curvature in the data of linewidth versus density is quite pronounced, but at low intensities it is absent. We also find it necessary to account for the Gaussian spatial distribution of the saturating electric field in our theory to obtain reasonable linewidths for measured experimental intensities. All of our experimental data have been fitted with this theory to obtain a power-broadening corrected value of the pressure-broadening coefficient for each perturber investigated. In general, the intensity-corrected value is ~20% greater than the uncorrected experimental result.

Comparison of our results with the data of other authors is limited to some extent by the small number of perturbers which they have investigated. Where comparison is possible our pressure-broadening results are generally (10–30)% larger for the 10.6-$\mu$m data and (30–70)% larger for the 9.6-$\mu$m data. Our results for $CO_2$, He, and $N_2$, however, provide the best agreement for the 9.6- and 10.6-$\mu$m gain measurements obtained by Alcock in high-pressure $CO_2$ amplifiers, a finding which lends strong support for the acceptance of these larger values. On the other hand, our broadening data do not reflect the rotational dependence found by other investigators involving *linear* measurements. The probable source of this result is attributable to an inadequate treatment of the saturation behavior of degenerate transitions including the effect of molecular reorientation.

Finally, we have appraised the character of the intermolecular forces involved in collisions between $CO_2$ and the various perturbers with the Murphy-Boggs theoretical linewidth formulation. With this analysis, originally developed for the microwave region, we have calculated the pressure-broadening coefficient in each case. Since the dominant interaction between $CO_2$ and the perturbers in the context of the MB theory is the quadrupole-quadrupole interaction, this analysis resulted in quadrupole moments for $CO_2$, $N_2O$, $N_2$, NO, CO, $O_2$, $H_2$, and $D_2$. It was observed that the quadrupole moments determined by this analysis differed by as much as a factor of four from alternative determinations. The differences between the theoretical and experimentally established values of the quadrupole moments of these molecules serve to highlight the inability of existing pressure-broadening theories to adequately treat the collision problem in this regime. In particular, it is evident that vibrational effects, especially where vibrational resonance is present, must be properly incorporated into the theoretical treatment.

## ACKNOWLEDGMENTS

The authors gratefully acknowledge many helpful conversations with P. W. Hoff, J. R. Murray, W. J. Stevens, C. Freed, F. R. Peterson, E. W. Smith, J. E. Boggs, T. Quist, and the expert technical assistance of B. R. Schleicher.

*Work performed under the auspices of the United States Atomic Energy Commission.

†Hertz Foundation Fellow, University of California, Dept. of Applied Science, Davis-Livermore, Cal. 94550. Current address: Air Force Weapons Laboratroy (LRL), Kirtland Air Force Base, N. M. 87117.

‡Paper based in part on material submitted by Thomas W. Meyer in Partial fulfillment of the requirements for the degree of Doctor of Philosophy at the University of Cal., Davis, Cal. 95616.

§Present address: Molecular Physics Center, Stanford Research Institute, Menlo Park, Calif. 94025.

[1]C. Freed and A. Javan, Appl. Phys. Lett. 17, 53 (1970).

[2]Other factors such as the radiative linewidth may also contribute to the width of the saturated resonance, but these are negligible in our case. See, for example, J. L. Hall, *The Lineshape Problem in Laser Saturated Molecular Absorption* (Institute for Theoretical Physics, University of Colorado, 1969).

[3]Our oscillators are similar to the designs of C. Freed at MIT's Lincoln Laboratory. C. Freed, IEEE J. Quantum Electron. QE-4, 404 (1968).

[4][C. Freed and A. Javan, Appl. Phys. Lett. 17, 53 (1970)] and B. J. Feldman [Ph.D. thesis, M.I.T., 1971 (unpublished)] have investigated the pressured dependence of the 4.3-$\mu$m saturated resonance. In June 1973 we become aware of the $CO_2$ work of F. R. Peterson at NBS Boulder. Peterson has observed the downward curvature in the low-pressure $CO_2$ broadening data.

[5]S. N. Bagaev, E. V. Boklanov, and V. I. Chebotaev, Zh. Eksp. Teor. Fiz. Piz'ma Red. 16, 15 (1972) [Sov. Phys.—JETP Lett. 16, 9 (1972)].

[6]The mode radius is defined as the $1/e^2$ point of intensity; cf. H. Kogelnik and T. Li, Appl. Opt. 5, 1550 (1966).

[7]W. E. Lamb, Jr., Phys. Rev. 139, A1429 (1964).

[8]S. Stenholm and W. E. Lamb, Jr., Phys. Rev. 181, 618 (1969).

[9]B. J. Feldman and M. Feld, Phys. Rev. A 1, 1375 (1970).

[10]H. K. Holt, Phys. Rev. A 3, 233 (1970).

[11]A. Szöke and A. Javan, Phys. Rev. Lett. 10, 521 (1963).

[12]S. G. Rautian, Zh. Eksp. Teor. Fiz. 15, 1176 (1966) [Sov. Phys.—JETP 24, 788 (1967)].

[13]B. L. Gyorffy, M. Borenstein, and W. E. Lamb, Jr., Phys. Rev. 169, 340 (1968).

[14]A. B. Kol'chenko and S. G. Rautian, Zh. Eksp. Teor. Fiz. 54, 959 (1968) [Sov. Phys.—JETP 27, 511 (1968)].

[15]A. B. Kol'chenko, S. G. Rautian, and R. I. Sokolovskii, Zh. Eksp. Teor. Fiz. 55, 1864 (1968) [Sov. Phys.—JETP 28, 986 (1969)].

[16]P. R. Berman and W. E. Lamb, Phys. Rev. A 2, 2435 (1970); 4, 319 (1971).

[17]C. Freed and H. A. Haus, IEEE J. Quantum Electron, QE-9, 219 (1973).

[18]V. N. Lisitsyn and V. P. Chebotaev, Zh. Eksp. Teor. Fiz. 54, 419 (1968) [Sov. Phys.—JETP 27, 227 (1968)]; V. S. Letokhov, *Proceedings of the Esfahan Symposium*, edited by M. S. Feld, A. Javan, and N. A. Kurnit (Wiley, New York, 1973).

[19]V. A. Alekseev, T. L. Andreeva, and I. I. Sobel'man, Zh. Eksp. Teor. Fiz. 64, 813 (1973) [Sov. Phys.—JETP 37, 413 (1973)].

[20]H. A. Haus and P. W. Hoff, MIT Quarterly Progress Report No. 93, 1969 (unpublished).

[21]H. Granek, C. Freed, and H. A. Haus, IEEE J. Quantum Electron. QE-8, 404 (1972).

[22]R. R. Jacobs, K. J. Pettipiece, and S. J. Thomas, Appl. Phys. Lett. 24, 375 (1974); IEEE J. Quantum Electron. QE-10, 480 (1974).

[23]E. R. Murray, C. Krager, and M. Mitchner, Appl. Phys. Lett. 24, 180 (1974). See also, D. W. Ducsik, B.S. thesis, M.I.T., 1968 (unpublished).

[24]T. K. McCubbin, Jr., R. Durone, and J. Sorrell, Appl. Phys. Lett. 8, 118 (1966).

[25]E. T. Gerry and D. A. Leonard, Appl. Phys. Lett. 8, 227 (1966).

[26]S. R. Drayson and C. Young, J. Quant. Spectrosc. Radiat. Transfer 7, 993 (1967).

[27]T. K. McCubbin, Jr., and T. R. Mooney, J. Quant. Spectrosc. Radiat. Transfer 8, 1255 (1968).

[28]D. E. Burch, D. A. Gryvnak, R. R. Patty, and C. E. Bartky, J. Opt. Soc. Am. 59, 267 (1969).

[29]A. D. Devir and U. P. Oppenheim, Appl. Opt. 8, 2021 (1969).

[30]C. Young, R. W. Bell, and R. E. Chapman, Appl. Phys. Lett. 20, 278 (1972).

[31]E. Arie, N. Lacombe, and C. Rossetti, Can. J. Phys. 50, 1800 (1972).

[32]E. Hoag (private communication). This was a joint effort by D. W. Ducsik (Ref. 5 of Chap. IV) and E. Hoag using the method of Ref. 25.

[33]The considerations of the "flywheel" model for rotational collisions serve to illustrate why the linewidth should decrease with increasing $J$. The energy spacings of the rigid rotator are $\sim BJ$, thus as $J$ increases, more energy is required to change the rotational state by one quanta. In collisions between two rotors, fewer inelastic events would occur at higher $J$'s, and therefore the linewidth would be narrower. For a theoretical analysis, see H. A. Rabitz and R. G. Gordon, J. Chem. Phys. 53, 1815 (1970); 53, 1831 (1970). Experimental results on high rotational states of $H_2O$ indicating anomalously low broadening are reported in R. S. Eng. A. R. Calawa, R. C. Harmon, P. L. Kelley, and A. Javan, Appl. Phys. Lett. 21, 303 (1972).

[34]One may argue in a qualitative manner that, if the effective dipole moment were to increase at lower values of $J$, then the effect of saturation should be more pronounced. A larger saturation contribution would appear to give the experimental data a shallower slope. The converse, of course, would be true at higher values of angular momentum. However, the small changes of the weighted dipole moment (Tables V–VI) have only a ~1% effect on the value of $1/\pi T_2$ found from the code MULT.

[35]See, for example, C. H. Townes and A. L. Schawlow, *Microwave Spectroscopy* (McGraw-Hill, New York, 1955), p. 21.

[36]Normally, the $m$ degeneracy of the states would not be a problem as long as they were separate unconnected levels. However, in the physical system we are studying, the $m$ levels are in fact connected by reorientational collisions. Thus, a proper theoretical treatment dictates the consideration of the influence of

these reorientation collisions in the presence of a saturating electric field.
[37]P. Goldreich, D. A. Keeley, and J. Y. Kwan, Astrophys. J. 174, 517 (1972).
[38]P. Goldreich, D. A. Keeley, and J. Y. Kwan, Astrophys. J. 179, 111 (1973).
[39]P. Goldreich, D. A. Keeley, and J. Y. Kwan, Astrophys. J. 182, 55 (1973).
[40]J. A. Alcock (private communication).
[41]At pressures in excess of 8 atm, Alcock's data deviate from the results of his model. This appears to be due to the possibility that the line shape may no longer be Lorentzian. See also, W. H. Christiansen, G. J. Mullaney, and A. Hertzberg, Appl. Phys. Lett. 18, 385 (1971); and N. Lacombe, C. Boulet, and E. Arie, Can. J. Phys. 51, 302 (1973).
[42]For a review of pressure-broadening theories, see G. Birnbaum, in *Advances in Chemical Physics*, edited by J. O. Hirschfelder (Interscience, New York, 1967), Vol. 12; and T. Oka, in *Advances in Atomic and Molecular Physics*, edited by D. R. Bates and I. Estermann (Academic, New York, 1973), Vol. 9.
[43]P. W. Anderson, Phys. Rev. 76, 647 (1949); C. J. Tsao and B. Curnutte, J. Quant. Spectrosc. Radiat. Transfer 2, 41 (1962).
[44]J. S. Murphy and J. E. Boggs, J. Chem. Phys. 47, 691 (1967).
[45]J. S. Murphy and J. E. Boggs, J. Chem. Phys. 47, 4152 (1967).
[46]J. S. Murphy and J. E. Boggs, J. Chem. Phys. 49, 3333 (1968).
[47]J. S. Murphy and J. E. Boggs, J. Chem. Phys. 50, 3320 (1969).
[48]Discussions of the various intermolecular forces are to be found in R. B. Bernstein and J. T. Muckerman, in *Advances in Chemical Physics*, edited by J. O. Hirschfelder (Interscience, New York, 1967), Vol. 12; A. D. Buckingham, in *Advances in Chemical Physics*, edited by J. O. Hirschfelder (Interscience, New York, 1967), Vol. 12, p. 107; and H. Margenau and N. R. Kester, *Theory of Intermolecular Forces* (Pergamon, New York, 1971), 2nd. ed.
[49]E. Smith (private communication).
[50]Krishnaji and S. L. Srivastava, J. Chem. Phys. 43, 1345 (1965).
[51]R. G. Gordon, J. Chem. Phys. 44, 3083 (1966).
[52]R. H. Tipping and R. M. Herman, J. Quant. Spectrosc. Radiat. Transfer, 10, 881 (1970).
[53]R. H. Tipping and R. M. Herman, J. Quant. Spectrosc. Radiat. Transfer, 10, 897 (1970).
[54]C. Boulet, P. Isnard, and A. Levy, J. Quant. Spectrosc. Radiat. Transfer, 13, 897 (1973).
[55]G. Yamamoto, M. Tanaka, and T. Aoki, J. Quant. Spectrosc. Radiat. Transfer 9, 371 (1969).
[56]C. Boulet, E. Arié, J. P. Boranich, and N. Lacombe, Can. J. Phys. 50, 2178 (1972).
[57]D. E. Stogryn and A. P. Stogryn, Mol. Phys. 11, 371 (1966).
[58]T. A. Dillon and J. R. Godfrey, Phys. Rev. A 5, 599 (1972).
[59]J. Manz, Mol. Phys. 6, 445 (1963).
[60]M. Girand, P. Robert, and L. Galatry, J. Chem. Phys. 53, 352 (1970).
[61]*Handbook of Chemistry and Physics*, edited by R. C. Weast (Chemical Rubber, Cleveland, 1972), 53rd. ed.
[62]J. O. Hirschfelder, C. F. Curtis, and R. B. Bird, *Molecular Theory of Gases and Liquids* (Wiley, New York, 1954).
[63]G. Yamamoto, M. Tanaka, and T. Aoki, J. Quant. Spectrosc. Radiat. Transfer 9, 371 (1969).
[64]C. Boulet, E. Arié, J. P. Boranich, and N. Lacombe, Can. J. Phys. 50, 2178 (1972).
[65]A. D. McClean, J. Chem. Phys. 38, 1347 (1963).
[66]M. Yoshmine (private communication).
[67]D. E. Stogryn and A. P. Stogryn, Mol. Phys. 11, 371 (1966).
[68]A. D. McClean and M. Yoshmine, J. Chem. Phys. 46, 3682 (1967).
[69]C. W. Scherr, J. Chem. Phys. 23, 569 (1956).
[70]M. Karplus and H. J. Kolker, J. Chem. Phys. 38, 1263 (1963).
[71]F. B. Billingsley and M. Krauss (private communication).
[72]W. M. Huo, J. Chem. Phys. 43, 624 (1965).
[73]R. K. Nesbet, J. Chem. Phys. 40, 3619 (1964).
[74]M. Kotani, Y. Mizuon, and K. Kagama, J. Phys. Soc. Jpn. 12, 707 (1957).
[75]W. Kolos and L. Wolniewicz, J. Chem. Phys. 41, 3674 (1964).
[76]M. Krauss (private communication).